MOLECULAR DYNAMICS SIMULATIONS OF ELECTRONIC PROPERTIES OF a-SiC/c-Si HETEROJUNCTIONS

V. I. Ivashchenko[*], P. E. A. Turchi[a], L. A. Ivashchenko

Institute of Problems of Materials Science, NAS of Ukraine, Krzhyzhanovsky Str. 3, 03680 Kyiv, Ukraine
[a]Lawrence Livermore National Laboratory (L-353), P.O. Box 808, Livermore, CA 94551, USA

Empirical molecular dynamics simulations combined with a recursion procedure are applied to study the atomic and electronic structures of a-SiC/c-Si heterojunctions. The heterojunctions are considered as the (001) silicon slabs covered with a-SiC thin films. The films are generated from the condensation of diluted Si-C vapour on the substrates similarly to the atom-by-atom deposition. One of the samples was annealed at different temperatures. The atomic and electronic properties of this sample were studied as a function of annealing temperature. The electronic structure was investigated. The main theoretical results on the a-SiC/c-Si structure are in rather good agreement with experimental data.

1. Introduction

Recent progress made in chemical vapour deposition (CVD), mainly plasma enhanced–CVD (PECVD), of hydrogenated amorphous silicon carbide (a-SiC:H) films hold promise for producing semiconductor devices based on a-SiC/c-Si heterojunctions [1]. The opto-electronic and microstructural properties of such heterojunctions have been widely studied [1-4]. It is well known that the semiconductor device performance strongly depends on film quality. Therefore, we will focus on the properties of the silicon carbide thin films grown on silicon substrates. In recent years, a growing interest arised in preparing unhydrogenated amorphous silicon carbide films (a-SiC) by using various techniques such as laser-ablation deposition (LAD), pulsed laser deposition, triode-sputtering deposition, r.f and dc magnetron sputtering, and arc deposition. The review of the works on the a-SiC films grown on various substrates was done in Refs. 5-7. This interest has been primarily motivated by the unique tribological properties of hydrogen-free films.

Hydrogen-free bulk silicon carbide was investigated theoretically in the framework of a first-principles pseudo-potential approach (PA)-molecular dynamics (MD) [8, 9] and tight binding (TB)-MD simulations [10,11]. In addition empirical potential (EP)-Monte Carlo (MC) simulations [12-14], EP-MD simulations [6,7,15-17] were used to study the atomic configurations and chemical ordering. The atomic and electronic structures of a-SiC:H were investigated with the help of the PA-MD [18], TB-MD [19] and EP-MC [14] simulations. Most a-SiC samples were generated by cooling the high-temperature 3C-SiC melt [8,9,12-17]. Both the TB 128-atom un-hydrogenated and hydrogenated samples were obtained from the diluted Si-C [10,11] and Si-C-H vapours [19]. The authors [20-23] have employed empirical MD simulations of displacement cascades under ion irradiation to study atomic arrangements in a-SiC. All the computational schemes mentioned above give similar sample characteristics. The main difference lies in the evaluation of the extent of chemical ordering. The structures with low chemical ordering were generated by using PA-MD and TB-MD simulations [8,10,11], whereas a-SiC samples with comparatively high chemical ordering were prepared by using techniques based on the empirical Tersoff potential [6, 7, 12-17, 20-23]. In contrast to the bulk a-SiC that has been widely studied with various theoretical and experimental procedures, no theoretical investigation of a-SiC films grown on a silicon substrate was yet carried out.

---

[*] Corresponding author: ivasch@materials.kiev.ua

To fill this gap, we have generated a series of a-SiC/c-Si hetero-structures representing condensed a-SiC thin films on a silicon slab. For this purpose, an atom-by-atom deposition scheme based on large-scale EP-MD simulations was proposed. Our motivation was based on the following facts. For various applications a-SiC/c-Si (a-SiC:H/c-Si) heterojunctions are produced by means of the deposition of the amorphous films on silicon crystalline wafers. The films are usually grown by vapour-growth or sputtering techniques. The atomic and electronic characteristics of the samples were thoroughly studied. An accent was put on the electronic structure investigations. The simulated film characteristics are compared with those obtained experimentally and theoretically on film and bulk a-SiC samples.

2. Computational aspects

A simulated sample consisting of 1344 atoms, i.e., 768 Si atoms belonging to a substrate and 576 atoms with an equal number of Si and C atoms belonging to SiC vapour in a $2.172 \times 2.172 \times 20.0$ nm rectangular cell is initially considered for MD simulations. The periodic boundary conditions along the x- and y- directions are taken into account. The film condensation is carried out with EP-MD simulations, in the constant number of particles-volume-temperature (NVT) ensemble, based on the Tersoff potential for SiC [12]. The simulation cell contains a substrate representing the lower (001) silicon slab having the (4×4×6) a_0 configuration (a_0 is the lattice parameter of c-Si), and an upper reservoir with the SiC diluted vapour. The vapour reservoir is thermostated to maintain the vapour at a specific temperature. It is displaced relatively to the substrate along the z-direction by a distance that exceeds the film thickness. A normal force directed towards the substrate is applied to each atom in the reservoir. The system is immovable due to the fixed lower substrate layer. The next six layers of the substrate are thermostated to control the substrate temperature. The controlled deposition parameters are: the vapour temperature (T_G), the normally applied particle force (F_N), and the substrate temperature (T_S). Each deposition is carried out during 22 ps, and after complete deposition a small amount of isolated atoms is found. Prior to deposition, the vapour and the substrate are equilibrated at T_G and T_S, respectively, for 5 ps. We have investigated the as-deposited films, i.e., the films that were not equilibrated after the deposition, and the relaxed samples that were equilibrated at temperatures equal to T_S during 50 ps and further cooled down to 300 K and equilibrated for 5 ps. Also, one sample was annealed at T_a=600, 1200, 2000 and 2500 K using both the NVT and NPT (constant number of particles-pressure-temperature) ensembles. In the NPT ensemble, we have applied the Andersen constant pressure method [24]. A mass for the external system that is required for the simulations [24] was set equal to the mass of all the atoms. When applied to the bulk a-SiC, the Andersen scheme gives an equilibrium volume at 300 K that differs by only 0.1% from that obtained from the simulations under constant bulk modulus (B=2.2 Mbar). All the equilibrated samples were relaxed for 5 ps. A time step of 1.0×10^{-15} s is used during all MD simulations.

In our investigation, a sp^3s^* TB scheme [25] is used to calculate the density of states (DOS) of a-SiC films. An analysis of the local DOS is carried out with the recursion technique described in Refs. 16,17. The initial cell is duplicated according to the periodic boundary conditions to generate a large cluster of ~5200 atoms. The local DOS of amorphous systems is obtained with 53 levels of continued fraction for the description of the one-electron Green function. This number of levels guarantees a convergence of the DOS for the corresponding crystalline materials [16, 17]. Our scheme gives BGs of 1.17, 2.40 and 5.50 eV for Si, 3C-SiC, and diamond, respectively, in close agreement with the experimental values. The scaling of the two-centre hopping parameters with inter-atomic distance is chosen according to the Harrison rule.

Following Fedders *et al.* [26], to clarify the extent of the localization of the electronic states, we define a "localized charge" q(n,E) associated with each eigenvalue with energy E and the atomic site centered on the atom number n. This charge is obtained from the eigenvectors of the TB matrix. The quantity q(n,E) summed over all atoms should be equal to unity, therefore it is not suitable for determining the localization of the electronic states at the energy E. For this reason a mean-square charge is introduced [26]

$$Q(E) = N \sum_n q(n,E)^2 \tag{1}$$

where N is the number of atoms in the sample. Given a distribution Q(E), the localization of a certain state can be evaluated by comparison with the initial charge distribution.

3. Results and discussion

A series of the samples was generated depending on the preparation conditions. The following deposition parameters were chosen: T_G=800, 1000, 1200, 1520, and 2000 K; F_N=0.05, 0.08, 0.10, 0.12, 0.15 nN; T_S=300, 600, 800, 1200, and 1520 K. Expecting a good heterostructure we have chosen the sample with most perfect atomic structure among other structures. This sample was defined in the following conditions: T_G=1200 K, F_N=0.1 nN and T_S=600 K (the sample abbreviation is 12-10-06). In Fig. 1 we show the atomic configuration in the sample. It is clearly seen that, after film condensation, the upper substrate layers undergo a distortion that leads to the formation of an amorphous region. The sample density as a function of the distance along the z-direction of the as-deposited and equilibrated samples generated in the NVT ensemble, N(Z), is shown in Fig. 2. The comparison between the densities N(Z) of the as-deposited and equilibrated samples shows that the substrate thickness increases after equilibration, which leads to reduced substrate density. In addition, in the relaxed samples, the amorphous region at the top of the substrate is narrower as compared to that in the as-deposited samples. From these results we deduce that the substrate in the as-deposited sample is under compressive stress.
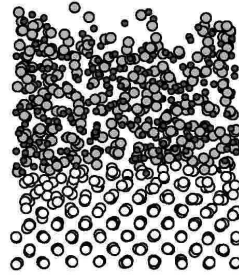

Fig. 1. Projections of atomic arrangements on the x-y plane of the as-deposited a-SiC film. The full circles correspond to the atoms in the films Si (large circles) and C (small circles). Only half of the substrate atoms is shown (open large circles).
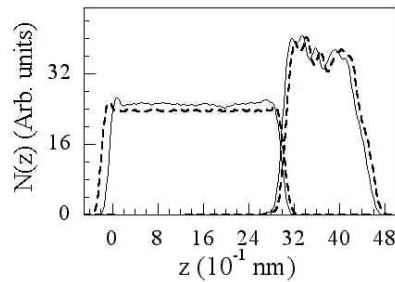

Fig. 2. Densities N(Z) of the as-deposited (solid line) and 600 K annealed (dashed line) samples in the NVT ensemble as a function of distance along the z-direction. The substrate extends up to ~3.2 nm.

Table 1. Percentage of three-fold, T_3, (n_3), four-fold, T_4, (n_4) atoms and i-j bonds (N_{i-j}), of the as-deposited and annealed 12-10-06 samples generated in the NVT and NPT ensembles.

Annealing temperature	Ensemble	n_3 (%)	n_4 (%)	N_{Si-Si} (%)	N_{Si-C} (%)	N_{C-C} (%)
	NVT (as-dep.)	27.6	55.7	20.1	58.3	21.6
600 K	NVT/NPT	25.0/24.8	55.4/55.9	21.2/21.6	57.8/57.4	21.0/21.1
1300 K	NVT/NPT	24.8/22.6	56.1/58.7	21.3/20.0	58.0/59.4	20.7/20.6
2000 K	NVT/NPT	23.4/21.7	62.2/63.5	18.3/18.8	60.1/60.2	21.6/21.0
2500 K	NVT/NPT	20.7/19.4	63.2/64.3	18.0/18.1	61.1/61.8	20.9/20.1

To clarify the nature of the structural transformation in a-SiC films under annealing conditions we investigated in detail the atomic configuration of the 12-10-06 sample annealed at 600, 1300, 2000, and

2500 K in the NVT and NPT ensembles. Structural characteristics of the annealed samples are given in Table 1. Note that all the structural parameters of the NVT and NPT films vary similarly with annealing temperature. An increase in annealing temperature leads to a noticeable increase in the number of four-fold coordinated (T_4) atoms and heteronuclear bonds. The C-C network is weakly changed with annealing temperature, and this can be attributed to the higher strength of the C-C bond energy compared to the energy of the Si-Si and Si-C interactions.

Together with improvements in the structural properties of annealed a-SiC films with increasing annealing temperature, reconstruction of the film surface occurs. Before annealing one void was observed at the centre of the as-deposited 12-10-06 film (not shown). The void spreads from the outer surface down to the substrate. An increase in T_a promotes atomic relaxation around the void, which leads to a decrease in the void volume and, when T_a is raised further, to its disappearance accompanied by an increase in the film density. This conclusion is consistent with the experimental observations [27]. Indeed, Höfgen *et al.* [27] examined the annealing behaviour of a-SiC using profilometry and x-ray diffraction, and observed large volume reduction of a-SiC prior to crystallization.
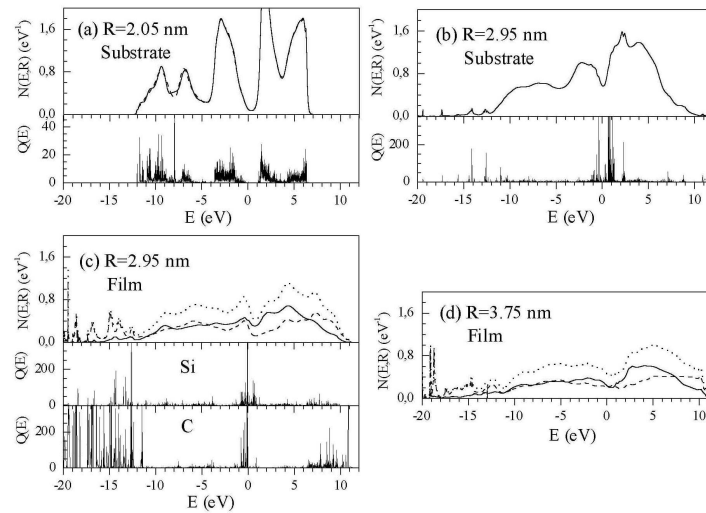

Fig. 3. Local layer-projected DOS N(E,R) associated with: (a) the middle of the substrate - N(E) obtained using a 1289 (solid line) and 5156 (dashed line) -atom cell; (b and c) the interface, and (d) the middle of the as-deposited 12-10-06 film: Si-projected DOS (solid line), C-projected DOS (dashed line) and total DOS (dotted line). R is the distance relative to the bottom of the substrate (see Fig. 2). Mean–square charge distribution Q(E) related to the (a) substrate DOS, and (b and c) and the interface DOS. The Fermi energy is located around 0.17 eV.

Typical layer-projected DOS associated with atoms located in the middle of the substrate, at the interface and in the middle of the 12-10-06 film are displayed in Fig. 3. The substrate DOS shows a distinct band gap around 0.0 eV (Fig. 3a). Although the interface and film DOS exhibit a trend toward band gap formation around 0.0 eV, a significant amount of deep states are present in the band gap region (Fig. 3b and c). It is well known that gap states are caused by coordination defects, strongly distorted T_4 sites, and homonuclear bonds [16, 17]. All these defects are present in both the interface and the film regions. The interface DOS is separated by the contributions from the substrate Si atoms (Fig. 3b), the film Si and C atoms (Fig. 3c). This gives us the possibility to analyse the DOS of silicon atoms belonging to the substrate and film in the interface region. It is seen from Fig. 3 that the electronic spectrum (b) is closer to the bulk DOS (a) than the Si projected partial DOS (c). It follows that the Si film atoms are distributed at the interface more randomly than the Si atoms belonging to the substrate. The pseudo-band gap around 0.0 eV becomes wider when going from the interface to the middle of the film, and this can be attributed to an increase in the number of C atoms in the nearest neighbor shells surrounding the Si atoms. The band-gap broadening is accompanied by the disappearance of the peak around –1.0 eV in the C projected DOS. This peak is assigned to C sp and sp^2 states [10, 11]. From this we deduce that the number of abnormally coordinated C atoms in the interface region is larger compared to that inside the film.

An important characteristic of the DOS is the extent of the electronic localization Q(E) over the range of the electronic spectrum. We see that, for the almost perfect electronic spectrum inside the

substrate, electronic states are weakly localized at the band edges (Fig. 3a). In the case of the substrate atoms at the interface, the strong electronic localization takes place at the bottom and at the top of the band gap (Fig. 3b). The states originated from the Si film atoms at the interface are localized mostly at midgap and at the bottom of the valence band (Fig. 3c). The carbon atoms located in the interface region give rise to strong electronic localization at the bottom of the valence band, in the band gap, and at the top of the valence band (Fig. 3c). We found a similar distribution of localized states for atoms located in the middle of the film (not shown). It follows that, regardless of the presence of a significant amount of gap states (that are associated with the interface and middle film regions) in the DOS, the film will exhibit semiconductor properties, since these states are strongly localized (correspondingly, they will not contribute to conductivity). On the other hand, they act as traps for carriers. To improve the opto-electronic properties of the films, deposition should be carried out from silicon and carbon containing precursors in the presence of hydrogen [1-4].
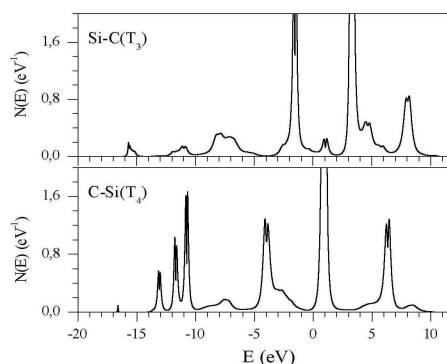

Fig. 4. Local DOS N(E) associated with single-fold coordinated Si and C atoms located on
the outer surface of the as-deposited sample.

By analogy with the hydrogen effect on dangling-bond states one would expect that the surface single-fold coordinated silicon or carbon atoms will be able to make the weak-bond passivation and will not give rise to gap states. As was mentioned above, the influence of other abnormally coordinated sites on the electronic spectrum was thoroughly examined earlier [10, 11, 16, 17]. Here, we present the results of the calculations of the local DOS associated with the single-fold coordinated Si and C atoms located on the outer film surface. In Fig. 4 we report the local DOS of such atoms belonging to as-deposited a-SiC films. It is seen that, in contrast with the expected results, both types of atoms give rise to gap states. The local DOS of the silicon atom in the Si-C(3) configuration and the carbon atom in C-Si(4) configuration exhibit distinct deep levels at the top of the band gap. Gap states having the C-origin are more localized than those caused by the Si atom in the single-fold coordinated configuration. A similar situation is observed for T_3 atoms (not shown). We expect that such circumstance is responsible for the single EPR signal with a g value of 2.0028 associated with the abnormally coordinated C atoms detected by Tabbal *et al.* in a-SiC films [5].
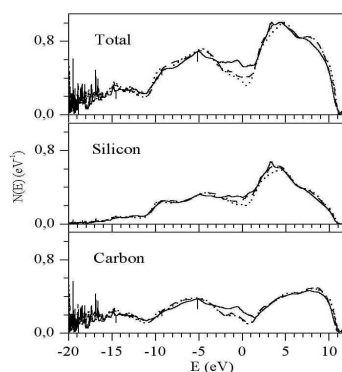

Fig. 5. Densities of states N(E) of the as-deposited (solid line), annealed at 2000 K (dashed
line) and 2500 K (dotted line) 12-10-06 samples in the NPT ensemble.

An increase in the Si-C hetero-nuclear bond density and some local ordering caused by annealing or modification of the deposition parameters leads to an improvement of the opto-electronic properties, and to a widening of the band gap in a-SiC films [5]. The observed variations of the electronic spectra of

as-deposited a-SiC films under annealing shown in Fig. 5 are consistent with this tendency. Upon annealing, the dip in the band gap region becomes deeper, and this is attributed to an improvement of the amorphous tetrahedral network. The band gap in the silicon projected DOS is formed in a narrow region around 0.0 eV, mostly due to a reduction of the Si dangling and homo-nuclear bonds. A change of the atomic configurations around the C atoms during annealing leads to the formation of a band gap in a wide energetic range. The peak around –1.0 eV in the carbon projected DOS, associated with sp- and sp^2-configurations, is reduced during annealing. This indicates that annealing promotes a reduction of the number of non-tetrahedral carbon configurations and leads to a widening of the band gap.

4. Conclusions

We have investigated the atomic and electronic structures of a-SiC/c-Si hetero-junctions. One sample was chosen to investigate the atomic configurations and electronic states. This as-deposited sample was further annealed. Sample annealing improves the tetrahedral network and, to a lesser extent, chemical ordering, by reducing the number of Si-Si homo-nuclear bonds. The compressive stress of the silicon substrate is expected to be significantly reduced upon annealing. The local densities of electronic states related to the interface atoms and to the film atoms exhibit a tendency towards band-gap formation. The single-coordinated atoms located on the outer surface give rise to gap states. The localization of the electronic states is highest in the band-gap region and at the band edges. The electronic localization is higher for carbon gap states than for silicon gap states. Upon annealing the semiconductor dip increases, and this is mostly attributed to a reduction in Si-Si homo-nuclear and C sp- and sp^2- configurations. The comparison between the computed characteristics and the analogous theoretical and experimental findings for bulk and film a-SiC and a-SiC:H samples validates our approach.

References

[1] J. Bullot, M. P. Schmidt, Phys. Stat. Sol. (b) **143,** 345 (1987).
[2] Proc. Inter. Conf. E-MRS, Strasbourg, Ed. L. Calcagno, A. Hallen, R. Martins, W. Skorupa, Elsevier, Amsterdam, The Netherlands, 2001, p. 528.
[3] D. Kruangam, T. Endo, M. Deguchi, W. Guang-Pu, H. Okamoto, Y. Hamakawa, Optoelectronics **1,** 67 (1986).
[4] Y. Hamakawa, Renewable Energy **15**, 22 (1998).
[5] M. Tabbal, S. Isber, T. C. Christidis, M. A. El Khakani, M. Chaker, J. Appl. Phys. **88,** 5127 (2000).
[6] M. Ishumaru, In-Tae Bae, Y. Hirotsu, S. Matsumura, K. Sickafus, Phys. Rev. Lett. **89**, 055502 (2002).
[7] S. Muto, T. Tanabe, J. Appl. Phys. **93**, 3865 (2003).
[8] F. Finocchi, G. Galli, M. Parrinello, C. M. Bertoni, Phys. Rev. Lett. **68**, 3765 (1992).
[9] P. C. Kelires, P. J. H. Denteneer, Solid State Commun. **87,** 851 (1993).
[10] V. I. Ivashchenko, P. E. A. Turchi, V. I. Shevchenko, L. A. Ivashchenko, G. V. Rusakov, Phys. Rev. B **66,** 195201 (2002).
[11] V. I. Ivashchenko, P. E. A. Turchi, V. I. Shevchenko, L. A. Ivashchenko, G. V. Rusakov, Diamond and Related Materials **12**, 993 (2003).
[12] J. Tersoff, Phys. Rev. B **49**, 16349 (1994).
[13] P. C. Kelires, Phys. Rev. B **46**, 10048 (1992).
[14] C. R. S. da Silva, J. F. Justo, A. Fazzio, Phys. Rev. B **65**, 104108 (2002).
[15] D. Mura, L. Colombo, R. Bertoncini, G. Mula, Phys. Rev. B **58**, 10357 (1998).
[16] V. I. Ivashchenko, V. I. Shevchenko, Appl. Surf. Sci. **184**, 137 (2001).
[17] V. I. Ivashchenko, V. I. Shevchenko, G. V. Rusakov, A. S. Klymenko, V. M. Popov, L. A. Ivashchenko, E. I. Bogdanov, J. Phys.: Condens. Matter **14**, 1799 (2002).
[18] F. Finoocchi, G. Galli, Phys. Rev. B **50**, 7393 (1994).
[19] V. I. Ivashchenko, P. E. A. Turchi, V. I. Shevchenko, L. A. Ivashchenko, G. V. Rusakov, J. Phys.: Condens. Matter **15**, 4119 (2003).
[20] F. Gao, W. J. Weber, Phys. Rev. B **63,** 054101 (2000).
[21] F. Gao, W. J. Weber, J. Appl. Phys. **89**, 4275 (2001).
[22] F. Gao, W. J. Weber, W. Jiang, Phys. Rev. B **63**, 214306 (2001).
[23] J. M. Perlado, L. Malerba, T. Diaz de la Rubia, Mater. Res. Soc. Symp. Proc. **540**, 171 (1999).
[24] H. C. Andersen, J. Phys. Chem. **72**, 2384 (1980).
[25] P. Vogl, H. P. Hjalmarson, J. D. Dow, J. Phys. Chem. Solids **46**, 365 (1983).
[26] P. A. Fedders, D. A. Drabold, Phys. Rev. B **47**, 13277 (1993).
[27] A. Hofgen, V. Heera, F. Eichhorn, W. Skorupa, J. Appl. Phys. **84**, 4769 (1998).